Right-Angle-Bent CPW for the Application of the Driver-Amplifier-Integrated 40 Gbps TW-EML Module

Ho-Gyeong Yun, Kwang-Seong Choi, Yong-Hwan Kwon, Joong-Seon Choe, Jong-Tae Moon, and Myung-Hyun Lee

ABSTRACT—In this letter we present a right-angle-bent coplanar waveguide (CPW) which we developed for the application of the driver amplifier-integrated (DAI) 40 Gbps traveling wave electroabsorption modulated laser module. The developed CPW realized parallel progression of the radio frequency (RF) and light using a dielectric overlay structure and wedge bonding on the bending section. The measured S_{11} and S_{21} of the developed CPW were kept below –10 dB up to 35 GHz and –3 dB up to 43 GHz, respectively. These measured results of the CPW were in good agreement with the simulation results and demonstrated the applicability of the CPW to the 40 Gbps communication module.

Keywords—Coplanar waveguide, 40 Gbps, dielectric overlay, wedge bonding.

I. Introduction

Recently, 40 Gbps transmission technology has been widely considered as a strong candidate for next-generation tera bps communication networks [1]. Therefore, it is crucial to secure state-of-the-art 40 Gbps optical components at low cost. In particular, 40 Gbps traveling-wave electroabsorption modulator-integrated DFB lasers (TW-EML) module has attracted much attention with its low chirp, low operating voltage, and low optical loss [2], [3]. In addition to the previous 40 Gbps TW-EML module, we are in developing a driver-amplifier-integrated (DAI) 40 Gbps TW-EML module. This system-on-package module includes a driver amplifier device, an EML device and a bias tee in a package. This hybrid integration is very attractive because its minimized footprint makes the 40 Gbps optical communication systems compact and cost-effective. Even though hybrid 10 Gbps EML modules with a driver amplifier are being produced, there has been no product and few reports on the DAI 40 Gbps TW-EML module.

In this letter, we present a right-angle-bent coplanar waveguide (CPW) which we developed for the fabrication of the DAI 40 Gbps TW-EML module. This newly developed CPW enabled the RF and light to progress in a parallel direction with only a minimal insertion loss by virtue of the dielectric overlay structure [4] at the bending section of the CPW. In addition, wedge bonding was also applied to the

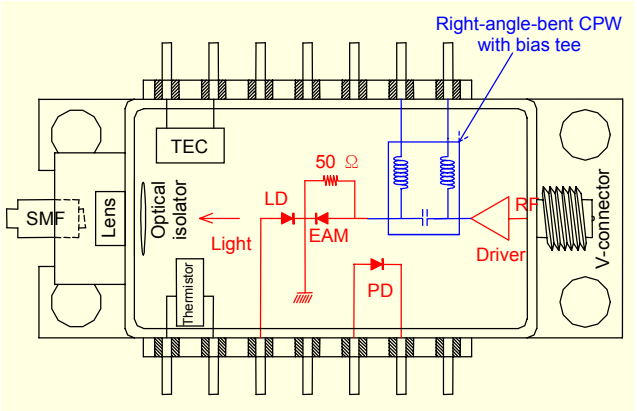

Fig. 1. Schematic drawing of the driver-amplifier-integrated 40 Gbps TW-EML module.

Manuscript received May 26, 2006; revised July 12, 2006.

Ho-Gyeong Yun (phone: +82 42 860 5017, email: yunhg@etri.re.kr), Kwang-Seong Choi (email: kschoi@etri.re.kr), Yong-Hwan Kwon (email: yhkwon@etri.re.kr), Joong-Seon Choe (email: jschoe@etri.re.kr), Jong-Tae Moon (email: jtmoon@etri.re.kr), and Myung-Hyun Lee (email: mhl@etri.re.kr) are with IT Convergence & Components Laboratory, ETRI, Daejeon, Korea.

CPW for the elimination of parasitic resonance. The CPW with this dielectric overlay structure and wedge bonding showed a large enough bandwidth for the application of the 40 Gbps communication module instead of a high cost chamfered structure with air-bridges [5], [6] .

In addition, a broadband bias tee composed of a conical inductor and a DC block capacitor was also integrated with this CPW. The return loss (S_{11}) and insertion loss (S_{21}) of the fabricated CPW were measured using a vector network analyzer before and after integration of the bias tee. These measured results were compared with the HFSS simulation results.

II. Design Concepts of the Right-Angle-Bent CPW

The integration of the bias tee on a transmission line and the parallel progression of RF and light are critical factors for the realization of compact and cost-effective 40 Gbps communication systems. In this letter, a CPW composed of Al_2O_3 (dielectric constant: 9.8, thickness: 0.635 mm) and Au metal patterns (thickness: 0.003 mm) was developed as a transmission line in consideration of the dimensions (0.5 × 1.0 mm) of a DC-block capacitor.

In the DAI 40 Gbps TW-EML module, the direction of the RF should be changed 90° for the parallel progression of RF and light. However, an abrupt CPW bending causes excessive capacitance, and excessive inductance and radiation because of the difference in path length between the inner and outer metallization slots [7].

To correct these unwanted loss factors at the abrupt-bent CPW, chamfered metal patterns and 3D air-bridges have been generally applied and the applicable bandwidth was acquired by this structure [8]. However, the fabrication of air-bridges on the upper surface of the CPW requires very complicated and high-cost manufacturing processes such as repeated photolithography [9] or micromachining [10]. In addition, the handling of the fabricated CPW with air-bridges (thickness: several μm) is also very difficult. Therefore, an additional protective layer [11], or special structures [12] are indispensable for the application of fabricated air-bridges. Consequently, the fabrication cost of a CPW with air bridges is 5 to 10 times higher than that of a CPW without air bridges.

For these reasons, a right-angle-bent CPW, which has a dielectric overlay structure at the bent section, was developed and simulated using HFSS. The dielectric overlay structure is fabricated by the partial removal of the conduction strip and the inner ground strip at the bending section [7]. This dielectric overlay structure makes the inner CPW mode progress more slowly than the outer CPW mode. Therefore, the phase distortion caused by the differences between the path length of the inner CPW and the outer CPW mode at the bending section is corrected with this dielectric overlay structure [4]. Figure 2 shows images of the developed CPW. While, the CPW with a bias tee has a gap in the middle of the signal plane for the attachment of the DC block capacitor, the CPW for S parameter measurement has no gap.

From the simulations, the developed CPW showed good transmission characteristics up to 32 GHz. However, a resonance peak appeared at about 32 GHz as shown in the circle pattern of Fig. 3. Figure 4(a) shows an asymmetrical propagation of the 2D electrical field of the top surface of the Al_2O_3 substrate at 32 GHz as a result of the resonance. In order to compensate this degradation, wedge bonding was applied between the two ground planes of the CPW instead of the conventional air-bridges. Wire bonding and ribbon bonding

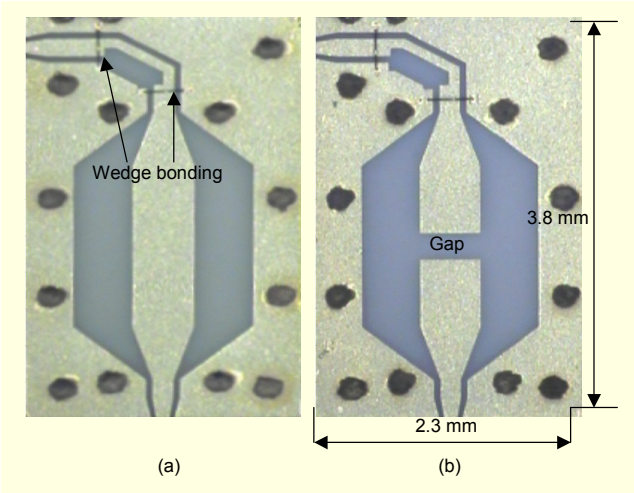

Fig. 2. The images of the developed CPW (a) without a gap in the middle of the signal line for S parameter measurement and (b) with a gap for the attachment of the DC-block capacitor.

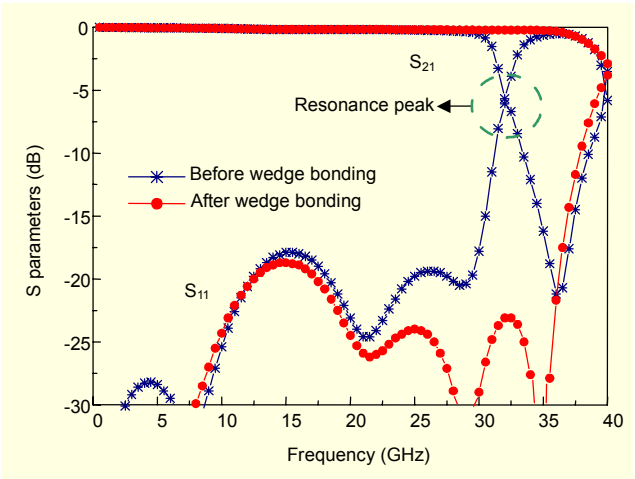

Fig. 3. The simulated S parameters of the CPW before and after applying wedge bonding to the CPW.

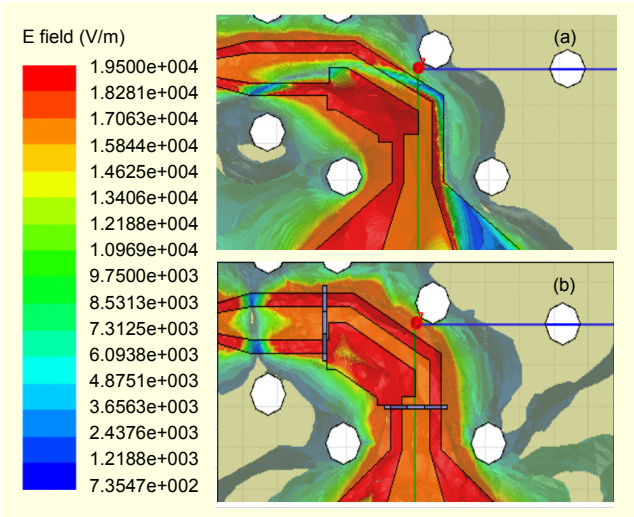

Fig. 4. 2D electrical field of the top surface of the Al_2O_3 substrate of the CPW at 32 GHz (a) before applying wedge bonding and (b) after applying wedge bonding.

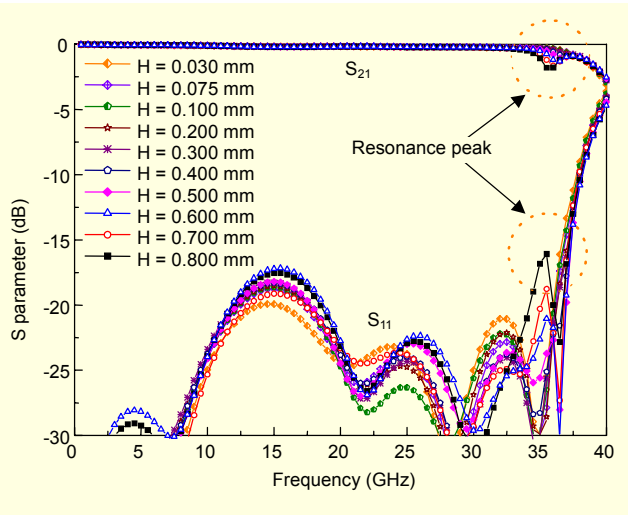

Fig. 5. The simulated S parameters of the CPW after applying wedge bonding to the CPW according to the wedge-bonding heights.

were also considered. However, the bonding wire had an asymmetrical shape between the first and second bonding and in using bonding ribbon it is difficult to control the shape. Therefore, wedge bonding, which is shown in Fig. 2(a), was selected as a compensation method. After applying the wedge bonding to the CPW, the resonance peak completely disappeared in the simulation as shown in Fig. 3. Figure 4(b) shows the clear propagation of the electric field at 32 GHz.

Furthermore, the CPW with wedge bonding proved that it has high enough tolerance for easy fabrication. Figure 5 shows the simulation results in terms of height. The simulation showed that the wedge-bonding heights from 0.03 mm to 0.4 mm have almost the same S parameters. When the height of the wedge-bonding was 0.5 mm, a resonance peak started to appear at about 35 GHz. Considering that the real wedge-bonding heights were 60±20 μm, this height of about 0.4 mm has high enough tolerance for easy fabrication of the wedge-bonding-applied CPW.

III. Measured Performances of the CPW

Figure 6 shows the measured S parameters of the developed CPW before and after applying wedge bonding to the CPW. A vector network analyzer was used to measure the S parameters. Before applying the wedge bonding, a resonance peak appeared at about 32 GHz, which is identical to the simulation results. However, the resonance peak completely disappeared after applying two wedge bondings to the CPW, and the S parameters did not depend on the height variance (60±20 μm) as the simulation results showed.

The measured S_{12} was kept over –3 dB up to 43 GHz and the

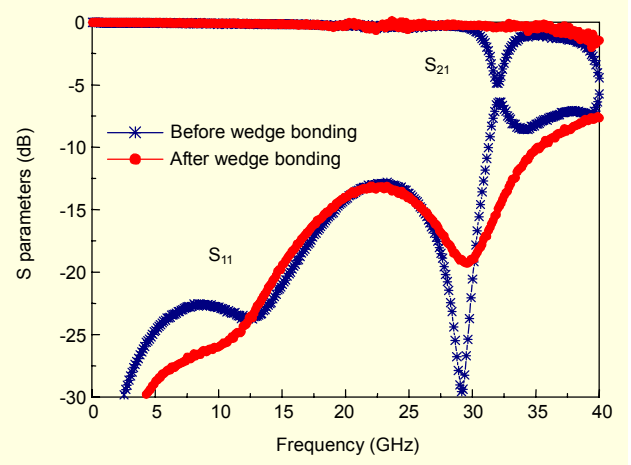

Fig. 6. Measured S parameters of the developed CPW before and after applying wedge bonding.

measured S_{11} was kept below –10 dB up to 35 GHz as shown in Fig. 6. These measured S parameters satisfied the requirements of the CPW for application in 40 Gbps communication modules because 40 Gbps communication systems generally use an NRZ coding system. In an NRZ coding system, if 3 dB bandwidth is over 30 GHz, the designed CPW is applicable to 40 Gbps modules [13].

To configure the bias tee on the CPW, a DC block capacitor and a broadband conical inductor were attached on the signal line of the CPW as shown in Fig. 7. After this integration of the passive components, the S parameters of the CPW with wedge bonding were also measured and the results are shown in Fig. 8. The measured S_{12} was kept over –3 dB up to 39 GHz and the measured S_{11} was kept below –10 dB up to 35 GHz.

Compared with the S parameters before integration of the passive components, these integrations only minimally degrade the transmission characteristics, which reflects inherent internal loss of the passive components.

These measured results of the developed CPW demonstrate the applicability of the CPW to a 40 Gbps communication module.

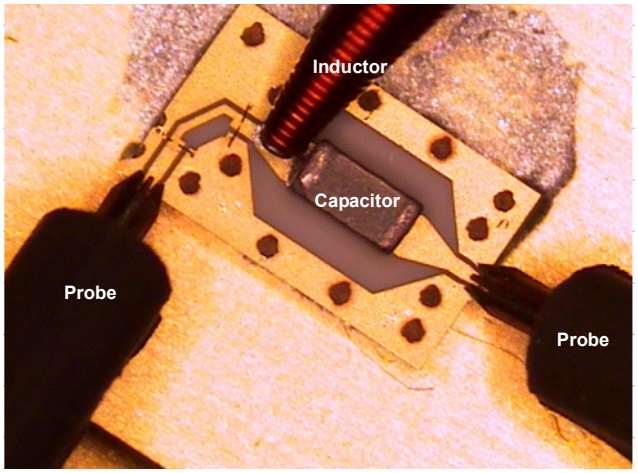

Fig. 7. Image of the developed CPW after integration of the inductor and capacitor for the bias tee.

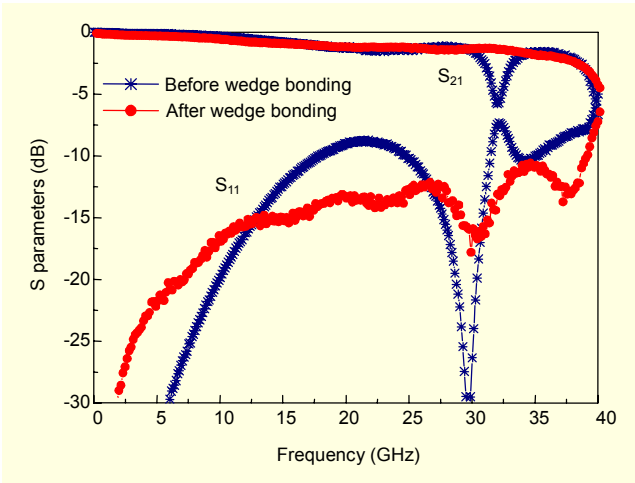

Fig. 8. Measured S parameters of the developed CPW with the integration of the passive components before and after wedge bonding.

IV. Conclusions

In this letter, we presented the right-angle-bent CPW which we developed for application to the DAI 40G TW-EML module, which is composed of an EML device and a driver amplifier in a module. The developed CPW with a dielectric overlay structure and wedge bonding showed a large enough bandwidth for application to a 40 Gbps communication module with a low-cost fabrication process. A bias tee was also integrated on the CPW with only minimal insertion loss and the measured S parameters of the CPW with a bias tee demonstrated its suitability for application to the DAI 40 Gbps TW-EML module.

References

[1] Y.H. Kwon, et al., "Fabrication of 40 Gb/s Front-End Optical Receivers Using Spot-Size Converter Integrated Waveguide Photodiodes," *ETRI J.*, vol. 27, 2005, pp. 484-490.

[2] H. Kawanishi, Y. Yamauchi, et al., "EAM-Integrated DFB Laser Modules with More than 40-GHz Bandwidth," *IEEE Photonics Tech. Letters*, vol. 13, 2001, pp. 954-956.

[3] K.S. Choi, et al., "Optimization of Packaging Design of TWEAM Module for Digital and Analog Applications," *ETRI J.*, vol. 26, 2004, pp. 589-596.

[4] R.N. Simons, G.E. Ponchak, "Modeling of Some Coplanar Waveguide Discontinuities," *IEEE Transactions on Microwave Theory and Tech.*, vol. 36, 1998, pp. 1796-1803.

[5] A.A. Omar, Y.L. Chow, "Effect of Air-Bridges and Mitering on Coplanar Waveguide 90° Bends: Theory and Experiment," *Microwave Symposium Digest*, vol. 2, 1996, pp. 823-826.

[6] T.M. Weller and R.M. Henderson, "Optimization of MM-Wave Distribution Networks Using Silicon-Based CPW," *Microwave Symposium Digest*, vol. 2, 1998, pp.7-12.

[7] R.N. Simons and G.E. Ponchak, "Channelized Coplanar Waveguide: Discontinuities, Junctions, and Propagation Characteristics," *IEEE MTT-S International*, vol. 3, 1989, pp.915-918.

[8] P.M. Watson and K.C. Gupta, "EM-ANN Modelling and Optimal Chamfering of 90° CPW Bends with Air-Bridges," *IEEE MTT-S International*, vol. 3, 1997, pp.1603-1606.

[9] S.A. Zaidel and T. and S. Alcorn, *Process for Making Air Bridges for Integrated Circuits,* US Patent 5408742, Martin Marietta Corporation, 1993.

[10] J.Y. Park, J.H. Sim, et al., "Fabrication of Thick Silicon Dioxide Air-Bridge for RF Application Using Micromachining Technology," *Microprocesses and Nanotechnology Conf.*, 2001, pp. 202-203.

[11] H.S. Cole Jr., et al., *Method for Making an Electronics Module Having Air Bridge Protection without Large Area Ablation*, US Patent 5548099, Martin Marietta Corporation, 2001.

[12] B. Gorowitz, C.A. Becker, et al., *Structure for Protecting Air Bridges on Semiconductor Chips from Damage*, US Patent 5,757,072, Martin Marietta Corporation, 1998.

[13] MAXIM High-Frequency/Fiber Communications Group, *NRZ Bandwidth - HF Cutoff vs. SNR*, Application Note, HFAN-09.0.1 (Rev. 0, 12/01), Dec. 2001, pp. 1-5.